Electrochimica Acta 54 (2009) 1070–1075

Contents lists available at ScienceDirect

Electrochimica Acta

journal homepage: www.elsevier.com/locate/electacta

Formation of anodic films on sputtering-deposited Al–Hf alloys

M. Fogazza[a], M. Santamaria[a], F. Di Quarto[a], S.J. Garcia-Vergara[b], I. Molchan[b], P. Skeldon[b,*], G.E. Thompson[b], H. Habazaki[c]

[a] Dipartimento di Ingegneria Chimica dei Processi et dei Materiali, Università di Palermo, Viale delle Scienze, Palermo 90128, Italy
[b] Corrosion and Protection Centre, School of Materials, The University of Manchester, P.O. Box 88, Manchester M60 1QD, UK
[c] Graduate School of Engineering, Hokkaido University, Sapporo 060-8628, Japan

ARTICLE INFO

Article history:
Received 4 July 2008
Received in revised form 7 August 2008
Accepted 28 August 2008
Available online 4 September 2008

Keywords:
Aluminium
Hafnium
Anodic oxidation

ABSTRACT

The growth of barrier-type anodic films at high efficiency on a range of sputtering-deposited Al–Hf alloys, containing from 1 to 95 at.% Hf, has been investigated in ammonium pentaborate electrolyte. The alloys encompassed nanocrystalline and amorphous structures, the latter being produced for alloys containing from 26 to 61 at.% Hf. Except at the highest hafnium content, the films were amorphous and contained units of HfO_2 and Al_2O_3 distributed relatively uniformly through the film thickness. Boron species were confined to outer regions of the films. The boron distributions suggest that the cation transport number decreases progressively with increasing hafnium concentration in the films, from ~0.4 in anodic alumina to ~0.2 for a film on an Al–61 at.% Hf alloy. The distributions of Al^{3+} and Hf^{4+} ions in the films indicate their similar migration rates, which correlates with the similarity of the energies of Al^{3+}–O^{2-} and Hf^{4+}–O^{2-} bonds. For an alloy containing ~95 at.% Hf, the film was largely nanocrystalline, with a thin layer of amorphous oxide, of non-uniform thickness, at the film surface. The formation ratios for the films on the alloys changed approximately in proportion to the hafnium content of the films between the values for anodic alumina and anodic hafnia, ~1.2 and 1.8 nm V^{-1} respectively.

1. Introduction

Studies of barrier-type anodic films formed on binary aluminium alloys are useful for understanding the influences of alloying elements during anodizing of commercial aluminium alloys. The resulting oxides, which incorporate units of aluminium oxide and alloying element oxide [1,2], usually in an amorphous film structure, are also of interest for investigation of band gap energies in "mixed" oxides [3]. They may also be of practical value due to their controllable dielectric constants. The oxides generally comprise single- or bi-layers depending upon the relative migration rates of the aluminium and alloying element ions in the oxide [4–6]. Similar migration rates of the two cation species lead to single-layered oxides, while differing migration rates result in an outer layer of the oxide of the faster migrating cation species. The oxides may also contain regions incorporating low concentrations of species derived from the anions in the electrolyte [7,8]. The outward migration of the cations is accompanied by inward migration of oxygen species [9]. Thus, the films form both at the metal/film and film/electrolyte interfaces and at the boundary between the inner and outer layers of layered films. The relative migration rates of the cation species usually show a dependence on the single metal–oxygen bond energies of the constituent oxide units, with species of high bond energy relative to Al^{3+}–O^{2-} migrating more slowly than Al^{3+} ions and vice versa [10,11]. Enrichment of the alloying element immediately beneath the oxide film may also occur when the Gibbs free energy of formation per equivalent for formation of the alloying element oxide is higher than that of alumina [6]. For alloys containing a sufficient level of alloying element in the bulk alloy, enrichment is not required for oxidation of the alloying element to proceed.

The present study investigates film formation on Al–Hf alloys prepared by magnetron sputtering. The primary interest here lies in the compositions of the anodic films and the migration behaviours of Al^{3+} and Hf^{4+} ions. The films may also be of interest as dielectrics, since hafnium oxide has attracted attention as a 'high-*K*' gate dielectric in metal oxide semiconductor transistors [12] and hafnia additions to alumina increase the dielectric constant [13–15].

2. Experimental

Al–Hf alloys were deposited by magnetron sputtering onto aluminium substrates, of dimensions 2.0 cm × 1.5 cm, using an Atom Tech System, with targets of 99.999% aluminium (Cu 0.3 ppm, Fe

* Corresponding author. Tel.: +44 161 306 4872; fax: +44 161 306 4826.
E-mail address: p.skeldon@manchester.ac.uk (P. Skeldon).

0013-4686/$ – see front matter © 2008 Elsevier Ltd. All rights reserved.
doi:10.1016/j.electacta.2008.08.052

0.3 ppm, Mg 1.2 ppm, Si 0.8 ppm) and 97.0% hafnium (Al 30 ppm, Cr < 50 ppm, Cu < 50 ppm, Fe 100 ppm, Mg < 10 ppm, Mo < 10 ppm, Nb < 50 ppm, Ta < 100 ppm, Ti 25 ppm, U 0.5 ppm, W < 50 ppm, Zr 2.8%, C 30 ppm, N 10 ppm). The aluminium substrates, which had been first electropolished and then anodized to form a 180 nm-thick barrier oxide films, were attached to a copper table that rotated beneath the targets. Deposition conditions were selected to provide alloys containing 1, 12, 26, 40, 54, 61, 95 at.% Hf. The alloy thicknesses were ~350 nm. Layers of aluminium and hafnium were also prepared, using the previous individual targets. The sputtering chamber was typically evacuated to $\sim 2 \times 10^{-5}$ Pa, with sputtering subsequently carried out in 99.999% argon at ~0.5 Pa. During deposition, the temperature of the copper table reached ~303 K. Specimens were also prepared from 99.99% aluminium sheet that was electropolished for 180 s in 20%/80% (by vol.) perchloric acid/ethanol at less than 278 K. Following masking, the various specimens were then anodized to 150 V at 5 mA cm^{-2} in 0.1 M ammonium pentaborate electrolyte at 293 K. Voltage–time responses were recorded during anodizing. Six specimens of each composition of material were individually anodized, with the average slope determined for the voltage–time response.

Ultramicrotomed sections of the deposited layers, prior to and following anodizing, were examined by transmission electron microscopy (TEM), in a JEOL FX 2000 II instrument. Compositions of alloys and anodic films were determined by Rutherford backscattering spectroscopy (RBS), using 2.0 MeV He^+ ions produced by the Van de Graff accelerator of the University of Paris. The ion beam, directed normal to the specimen surface, was of 1 mm diameter, with scattered ions detected at 165° to the direction of the incident beam. The data were interpreted using the RUMP program [16]. Distributions of aluminium, hafnium, oxygen and boron through the anodic film thicknesses were analysed by glow-discharge optical

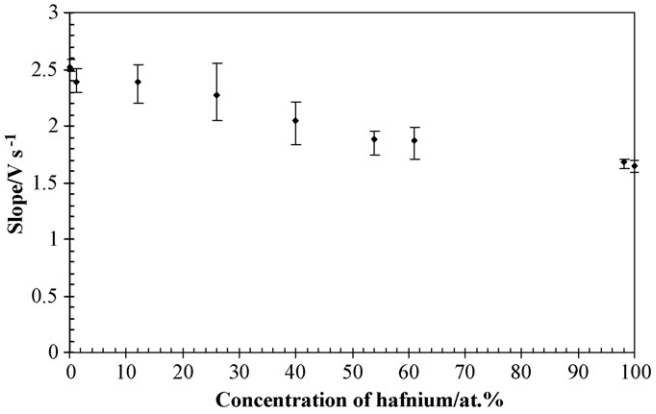

Fig. 1. The dependence of the slope of the voltage–time response on the composition of the substrate for anodizing of aluminium, hafnium and Al–Hf alloys at 5 mA cm^{-2} in 0.1 M ammonium pentaborate electrolyte at 293 K.

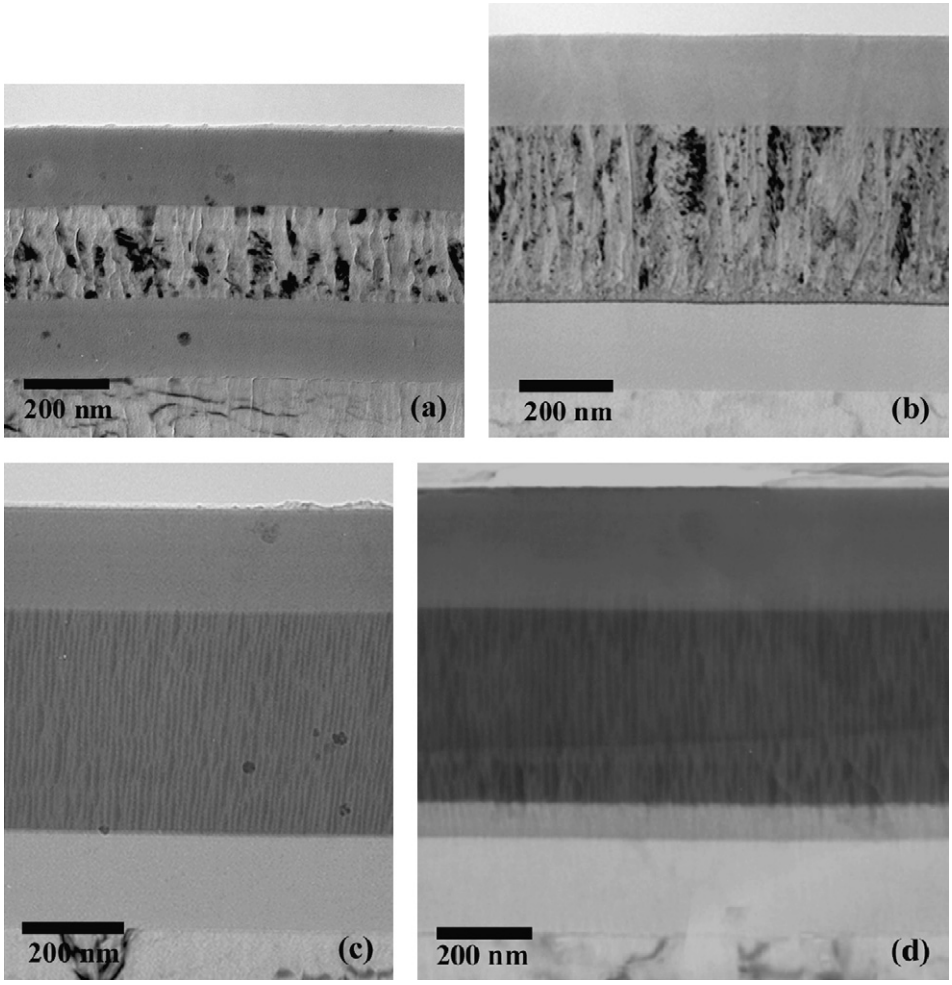

Fig. 2. Transmission electron micrographs of ultramicrotomed sections of Al–Hf alloys anodized at 5 mA cm^{-2} in 0.1 M ammonium pentaborate electrolyte at 293 K. (a) Al–1 at.% Hf; (b) Al–12 at.% Hf; (c) Al–26 at.% Hf and (d) Al–61 at.% Hf.

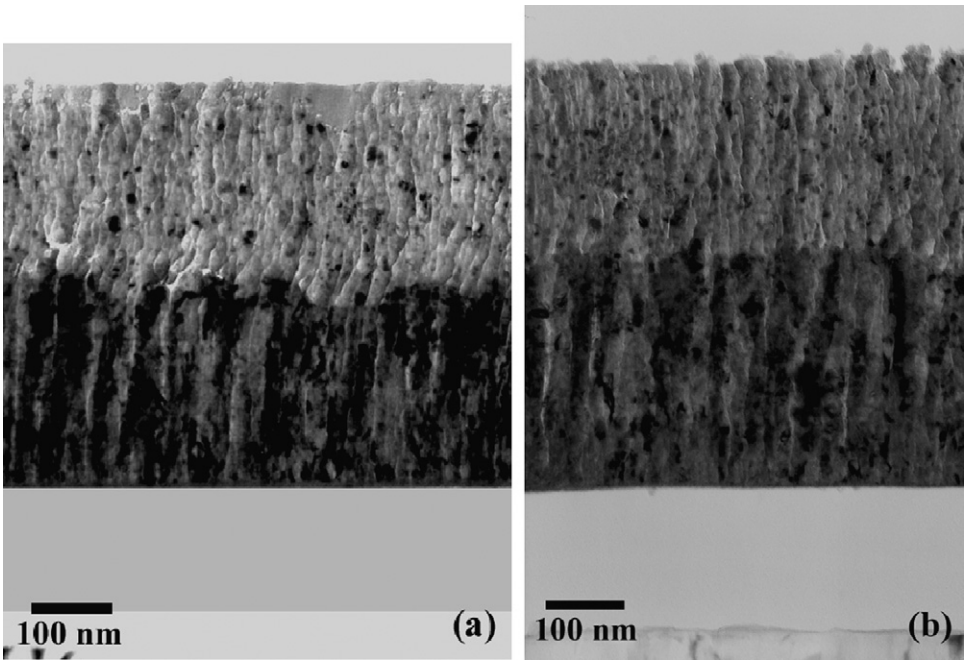

Fig. 3. Transmission electron micrographs of ultramicrotomed sections of (a) Al–95 at.% Hf alloy and (b) hafnium anodized at 5 mA cm^{-2} in 0.1 M ammonium pentaborate electrolyte at 293 K.

emission spectroscopy (GDOES), using a GD-Profiler (Horiba Jobin Yvon) operating at 13.56 MHz. A 4-mm copper anode and argon gas were employed for generation of the plasma. Sputtering was carried out at an argon pressure of 750 Pa and power of 35 W. The responses from the sputtered elements, other than hafnium, were detected with a polychromator of focal length of 500 mm. For detection of hafnium, a monochromator adjusted for the hafnium line at 263.872 nm was used.

3. Results

Fig. 1 presents the slopes of the linear voltage-time responses for anodizing of the alloys; the slopes reduced with increasing amounts of hafnium. Transmission electron micrographs of Fig. 2 show ultramicrotomed sections of anodized Al–Hf alloys, containing from 1 to 61 at.% Hf, revealing amorphous anodic films of uniform thickness. The occasional crystals in the film formed on the Al–1 at.% Hf alloy were formed due to electron irradiation during TEM. The films formed on the Al–40 at.% Hf and Al–54 at.% Hf are not shown, since these were similar to that on the Al–61 at.% Hf alloy. The featureless appearance of alloys containing from 26 to 61 at.% Hf suggest amorphous structures, contrasting with the nanocrystalline layers containing 1 and 12 at.% Hf. The films appear to be mainly uniform in composition. However, the slightly lighter appearance of an outer layer of some of the amorphous films, which is evident in micrographs for alloys containing from 26 to 61 at.% Hf, suggests the presence of boron species. The incorporation of boron species into the outer regions of the films was confirmed in elemental depth profiles determined using GDOES, which are shown later. The thickness of the boron-containing layer reduces with increasing hafnium concentration, representing ~0.22, 0.24, 0.27 and 0.35 of the film thickness for alloys containing 61, 54, 40 and 26 at.% Hf respectively. For alloys with lower hafnium contents, the contrast was too weak to be resolved. However, it is well established that anodic alumina films formed under the present conditions contain boron species in the outer ~0.40 of the film thickness in amounts of ~1 at.% [17].

The anodic films formed on the 95 and 100 at.% Hf layers, shown in Fig. 3, were nanocystalline and less uniform in thickness than the previous amorphous films. With the 95% Hf alloy, small regions of amorphous material were present near the film surface. These regions were typically ~10–20 nm thick, but with local thickness extending to ~50 nm. The anodic films formed on the electropolished and sputtering-deposited aluminium specimens were amorphous, as expected from previous work [11], and of similar thickness. From the thicknesses of the anodic films and the final anodizing voltage, namely 150 V, the formation ratios were derived; Fig. 4 discloses a linear trend with alloy composition, rising from ~1.2 nm V^{-1} for aluminium to ~1.8 nm V^{-1} for hafnium.

The RBS spectra for the alloys could be fitted using uniform film compositions comprising units of Al_2O_3 and HfO_2 in proportion to the atomic ratio of Al/Hf in the substrate; typical spectra are shown in Fig. 5. Efficiencies of close to 100% were indicated by the charge of the cations in the film compared with the charge passed during anodizing (Table 1). The relatively uniform presence of aluminium

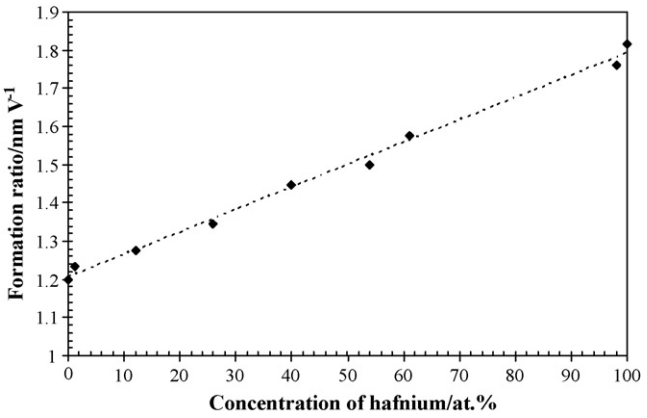

Fig. 4. The dependence of the formation ratio on the composition of the substrate for anodizing of aluminium, hafnium and Al–Hf alloys at 5 mA cm^{-2} in 0.1 M ammonium pentaborate electrolyte at 293 K.

Table 1
Compositions of oxide films used in fitting of RBS spectra and efficiencies of anodizing determined from the ratio of the charge of the cations in the film and the charge passed during anodizing

Concentration of Hf in alloy (at.%)	Hf in the oxide (atoms cm^{-2})	Al in the oxide (atoms cm^{-2})	Cation charge (C cm^{-2})	Charge passed during anodizing (C cm^{-2})	Efficiency (%)
1.1	0.07×10^{17}	6.14×10^{17}	0.29	0.30	100
12	0.77×10^{17}	5.66×10^{17}	0.32	0.33	100
26	1.63×10^{17}	4.63×10^{17}	0.33	0.33	99
40	2.44×10^{17}	3.66×10^{17}	0.33	0.35	94
54	3.21×10^{17}	2.74×10^{17}	0.34	0.36	94
61	3.77×10^{17}	2.41×10^{17}	0.36	0.38	95
95	7.20×10^{17}	0.36×10^{17}	0.48	0.48	100

The accuracy of the analyses is ~5%.

and hafnium in the films and the high efficiency of film formation are consistent with similar rates of migration of Al^{3+} and Hf^{4+} ions in the films. RBS is insensitive to low amounts of boron in the anodic films.

GDOES depth profiling confirmed the distribution of aluminium and hafnium species throughout the film thicknesses and the presence of boron species in outer regions of the anodic film; typical elemental depth profiles are shown in Fig. 6. The oscillations in the signals for aluminium and hafnium in the film are due to optical interference. The thickness of the film region containing boron relative to the film thickness was determined from the ratios of the time of sputtering of the boron-containing region, measured at the half-heights of the boron signals, compared with the time of sputtering of the oxide, measured at half-heights of hafnium, aluminium and oxygen signals, at locations corresponding to the film surface and alloy/film interface. Fig. 7 shows that the relative thicknesses of the boron-containing region increased with reducing hafnium content of the film from ~0.19 for the alloy containing 5 at.% Al to ~0.45 for the alloy containing 1 at.% Hf. The respective values were close to those indicated for anodic films formed on hafnium and aluminium, ~0.18 and ~0.43. However, the boron signal for the film formed on hafnium was ~50% lower than that for the Hf–5 at.% Al alloy. The line in Fig. 7 shows the linear relationship for the boron distribution in the amorphous films. The relative thicknesses of the boron-containing layers were in good agreement with values determined from atomic number–thickness contrast in the TEM, indicating that sputtering rates were not significantly affected by the presence of boron in the outer film regions.

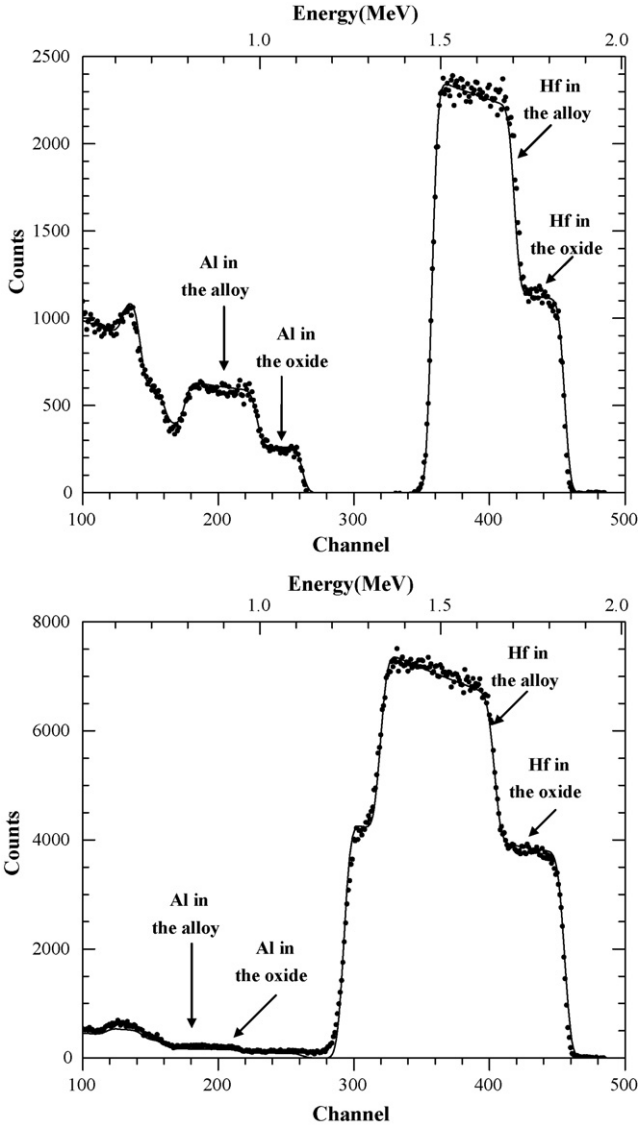

Fig. 5. Experimental and simulated (solid line) RBS spectra for (a) Al–12 at.% Hf and (b) Al–61 at.% Hf alloys anodized at 5 mA cm^{-2} in 0.1 M ammonium pentaborate electrolyte at 293 K.

4. Discussion

The gradients of the voltage–time responses for the sputtering-deposited aluminium and hafnium are $\sim 2.52 \pm 0.04$ and 1.65 ± 0.05 V s^{-1} respectively. The gradient for the bulk aluminium was 2.30 ± 0.01 V s^{-1}. Respective gradients of 2.35 and 1.56 V s^{-1} are calculated for formation of oxide at 100% efficiency, using Faraday's law and densities of 3.1 [18] and 9.68 g cm^{-3} [19] and the present formation ratios of ~1.2 and 1.8 nm V^{-1} for alumina and hafnia respectively. Previously, a formation ratio of 2.0 nm V^{-1} has been reported for anodic hafnia [20]. The measured values for the sputtering-deposited substrates are ~7% and 6% higher than the calculated values for alumina and hafnia respectively, and for the bulk aluminium substrate within 3% of the calculated value. The gradients for the alloys, shown in Fig. 1, were approximately equal to sum of those of the pure metals weighted according to the alloy composition. The gradients of the voltage–time responses are consistent with film formation at high efficiency.

Amorphous anodic oxides are produced for alloys containing up to at least 61 at.% Hf, with relatively uniform films, consisting of units of Al_2O_3 and HfO_2. The films contain small amounts of boron in the outer regions. Boron species are immobile in anodic alumina [17], which correlates with the high energy of the B^{3+}–O^{2-} relative to that of the Al^{3+}–O^{2-} bond, namely ~526 and ~281 kJ mol^{-1} respectively. Immobility of boron species is expected in amorphous hafnia, since the bond energy of B^{3+}–O^{2-} also exceeds that of Hf^{4+}–O^{2-}, the latter being ~284 kJ mol^{-1}. Thus, the boron-contaminated region of the film is presumed to be formed by

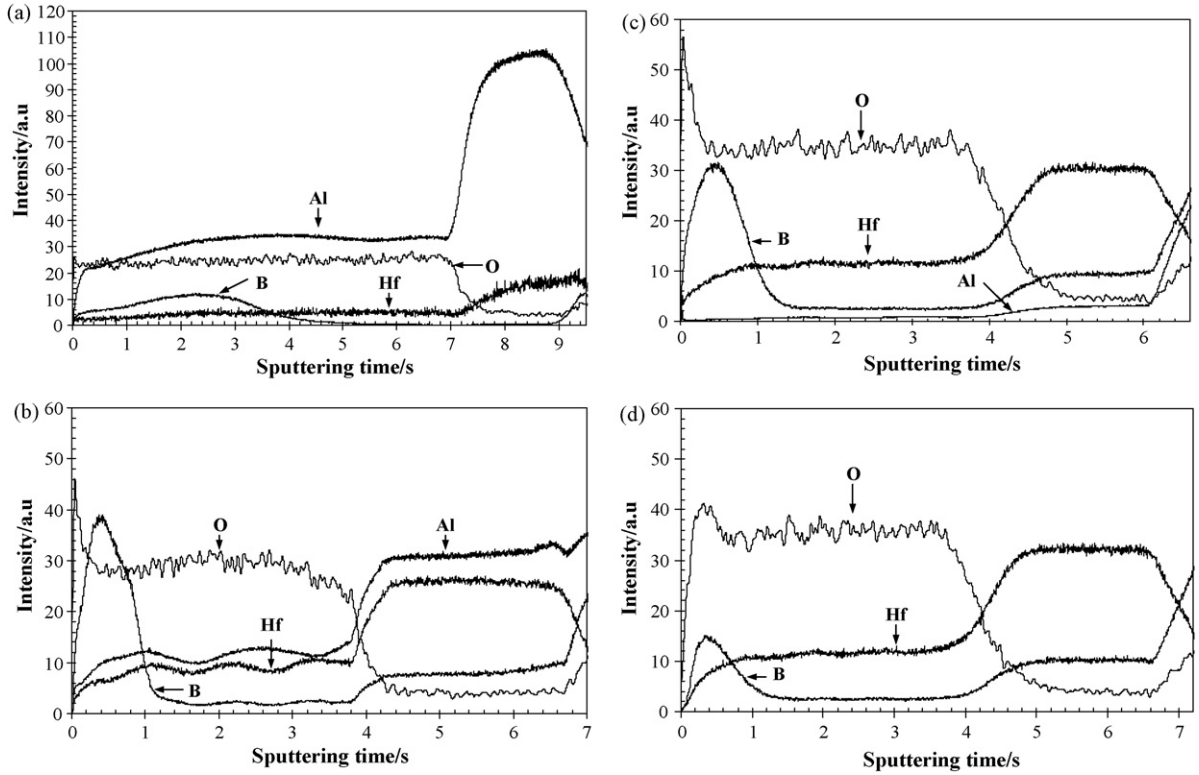

Fig. 6. GDOES elemental depth profiles for (a) Al–1 at.% Hf; (b) Al–61 at.% Hf; (c) Al–95 at.% Hf and (d) hafnium anodized at 5 mA cm^{-2} in 0.1 M ammonium pentaborate electrolyte at 293 K.

outward migration of Al^{3+} and Hf^{4+} ions. The outward migrating cations form amorphous oxide incorporating units of Al_2O_3 and HfO_2, in addition to a low concentration of boron species. The remainder of the film forms at the alloy/film interface due to inward migration of O^{2-} ions. The approximate cation transport number is indicated by the relative thickness of the boron-contaminated region. For the present films, the cation transport number decreases with increasing hafnium content of the film, from 0.45 for the film on the Al–1 at.% Hf alloy to 0.22 for the film on the Al–61 at.% Hf alloy. The former value is not significantly different from the value found for anodic alumina, about 0.44, which is also consistent with findings using a xenon marker [21]. The Al–Hf alloys prepared by magnetron sputtering revealed either nanocrystalline or amorphous structures depending upon their composition. Amorphous alloys were produced for compositions from 26 to 61 at.% Hf. However, the growth of the amorphous anodic films appeared to negligibly affected by the structure of the underlying alloy. The relation between cation transport number and film, or alloy, composition, shown in Fig. 7, is approximately linear for the amorphous anodic films, with extrapolation indicating a cation transport number of ~0.05 for amorphous anodic hafnia.

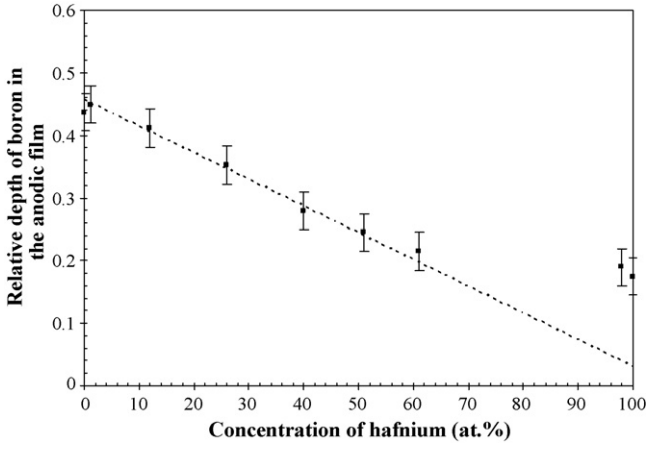

Fig. 7. The dependence of the relative depth of boron in the anodic film (depth of boron-containing layer to total film thickness, determined by GDOES) on the composition of the substrate for anodizing of aluminium, hafnium and Al–Hf alloys at 5 mA cm^{-2} in 0.1 M ammonium pentaborate electrolyte at 293 K.

The Gibbs free energy per equivalent for the formation of HfO_2 and Al_2O_3 are similar, namely −272.1 and −263.7 kJ mol^{-1} respectively [19], suggesting little or no enrichment of hafnium in the alloy immediately beneath the anodic film [6]. Any enrichment should be most noticeable by RBS in analyses of the Al–1 at.% Hf alloy, due to the relatively low signal from the hafnium in the bulk alloy. However, neither a peak in the hafnium yield, due to the enrichment at the alloy/film interface, or shift in the leading edge of hafnium, due to the initial formation of a hafnium-free anodic film, were resolved, indicating an upper limit on the enrichment of 5×10^{14} Hf atoms cm^{-2}. GDOES was also unable to detect the enrichment.

The similarity of the distributions of Al^{3+} and Hf^{4+} ions in the anodic films, together with film growth at high efficiency, indicates that the migration rates of Al^{3+} and Hf^{4+} ions are similar, which is consistent with their respective bond energies with oxygen. The migration rates of Al^{3+} and Hf^{4+} ions do not change significantly over a wide range of film composition. In a study of an Al–Zr alloy, similar migration rates were also found for Al^{3+} and Zr^{4+} ions [22], while a relatively low cation transport number of ~0.15 was suggested for amorphous anodic zirconia from studies of Ti–Zr alloys [23]. The relative migration rates of the cation species clearly do not correlate with their ionic charges, which would suggest a faster migration of Hf^{4+} ions than of Al^{3+} ions. Nor do they correlate with

ionic radii of Al^{3+} and Hf^{4+} ions, with respective values of 0.39 and 0.58 nm for four-fold co-ordination and 0.535 and 0.71 nm for six-fold co-ordination. Various models of ionic migration have been proposed ranging from early suggestions of vacancy diffusion and interstitial exchange capture [24] to a liquid-droplet mechanism [25] that allows for counter-migration of anions and cations with similar transport number. A more recent model links the migration of cations to structural relaxation around oxygen vacancies [26].

The anodic films formed on hafnium and the Al–95 at.% Hf alloy, were nanocrystalline. However, the film on the latter contained amorphous regions at the film surface. In common with nanocrystalline zirconia, nanocrystalline hafnia forms primarily by inward migration of O^{2-} ions, with a cation transport number of <0.05 [27]. Thus, anodic hafnia forms largely at the metal/film interface by transport of oxygen along short-circuit paths through the oxide. However, for the Al–95 at.% Hf alloy, initial formation of amorphous oxide is suggested, followed by transition to growth of nanocrystalline material. The initially formed amorphous oxide remains at the film surface. The amorphous region extends to depths of up to ~0.18 of the film thickness, which is similar to the depth distribution of boron determined by GDOES. Boron species may reside primarily in the amorphous regions, since the film formed on hafnium in which amorphous oxide was not resolved contained much less boron. For the mainly nanocrystalline films, the distribution of boron may therefore not be an indicator of the proportion of film growth due to cation transport. Ionic transport within the amorphous layer is presumed to supply oxygen ions to the underlying hafnium-rich oxide. In studies of Ti–Zr alloys, amorphous anodic films underwent a structural transition for sufficiently high zirconium contents, with ~63 at.% Zr promoting generation of nanocrystals of zirconia [23]. The nanocrystals were distributed within the inner, mainly amorphous, layer formed due to inward migration of O^{2-} ions. A similar type of mixed film structure may arise for Al–Hf alloys for compositions between 61 and 95 at.% Hf, prior to generation of the nanocrystalline oxide of high hafnium content.

5. Conclusions

Anodic films formed on sputtering-deposited Al–Hf alloys at 5 mA cm^{-2} in 0.1 M ammonium pentaborate electrolyte at 293 K comprise units of Al_2O_3 and HfO_2 distributed throughout the film thickness. The films are amorphous on alloys containing up to at least 61 at.% Hf, with transition to mainly nanocrystalline material at high hafnium contents. The growth of the amorphous anodic films appeared to negligibly affected by the structure of the underlying alloy.

The relative uniformity of the composition of the amorphous oxides is consistent with growth by inward migration of O^{2-} ions and outward migration of Al^{3+} and Hf^{4+} ions at similar rates. The cation transport number in the amorphous oxides reduces with increase of hafnium content. For high hafnium contents, the films are nanocrystalline.

The formation ratios increased linearly with increasing hafnium content of the anodic films, from 1.2 nm V^{-1} for anodic alumina to 1.8 nm V^{-1} for anodic hafnia. The transport number of cations in the amorphous films also shows a linear trend from ~0.4 for alumina to ~0.2 for the film on an Al–61 at.% Hf alloy. Extrapolation suggests a cation transport number of ~0.05 in amorphous anodic hafnia.

Acknowledgements

The authors are grateful to the Engineering and Physical Sciences Research Council (U.K.) for support of this work. They also wish to thank Dr I. Vickridge, Universités Paris 7 et 6, for assistance with ion beam analyses.

References

[1] K. Sasaki, T. Umezawa, Thin Solid Films 74 (1980) 83.
[2] V. Labunov, V. Sokol, A. Vorobiova, V. Bondarenko, Electrochim. Acta 30 (1985) 1079.
[3] N.T.C. Oliveira, S.R. Biaggio, S. Piazza, C. Sunseri, F. Di Quarto, Electrochim. Acta 49 (2004) 4563.
[4] H. Habazaki, K. Shimizu, P. Skeldon, G.E. Thompson, G.C. Wood, J. Mater. Res. 12 (1997) 1885.
[5] H. Habazaki, K. Shimizu, P. Skeldon, G.E. Thompson, G.C. Wood, J. Electrochem. Soc. 143 (1996) 2465.
[6] H. Habazaki, K. Shimizu, P. Skeldon, G.E. Thompson, G.C. Wood, X. Zhou, Trans. Inst. Met. Finish. 75 (1997) 18.
[7] H. Takahashi, K. Fujimoto, M. Nagayama, J. Electrochem. Soc. 135 (1988) 1349.
[8] H. Konno, S. Kobayashi, H. Takahashi, M. Nagayama, Electrochim. Acta 25 (1980) 1667.
[9] L. Iglesias-Rubianes, P. Skeldon, G.E. Thompson, H. Habazaki, K. Shimizu, Corros. Sci. 45 (2003) 2905.
[10] G. Alcala, S. Mato, P. Skeldon, G.E. Thompson, K. Shimizu, H. Habazaki, Corros. Sci. 45 (2003) 1803.
[11] H. Habazaki, K. Shimizu, P. Skeldon, G.E. Thompson, G.C. Wood, Corros. Sci. 43 (2001) 1393.
[12] Y.H. Kim, J.C.-Y. Lee, J.C. Lee, S. Banerjee, Hf-based High-*k* Dielectrics: Process Development, Morgan & Claypool, 2005.
[13] H.Y. Yu, M.F. Li, B.J. Cho, C.C. Yeo, M.S. Joo, D.-L. Kwong, J.S. Pan, C.H. Ang, J.Z. Zheng, S. Ramanathan, Appl. Phys. Lett. 81 (2002) 376.
[14] J. Petry, W. Vandervorst, T. Conard, Mater. Sci. Eng. B 109 (2004) 56.
[15] O. Buiu, Y. Lu, S. Hall, I.Z. Mitrovic, R.J. Potter, P.R. Chalker, Thin Solid Films 515 (2007) 3772.
[16] L.R. Doolittle, Nucl. Instrum. Methods B9 (1985) 344.
[17] K. Shimizu, G.E. Thompson, G.C. Wood, Thin Solid Films 85 (1981) 53.
[18] P. Skeldon, K. Shimizu, G.E. Thompson, G.C. Wood, Surf. Interface Anal. 5 (1983) 247.
[19] D.R. Lide, Handbook of Physics and Chemistry, 78th ed., CRC Press, Boca Raton, NY, 1997–1998.
[20] M.T. Thomas, J. Electrochem. Soc. 117 (1970) 396.
[21] F. Brown, W.D. Mackintosh, J. Electrochem. Soc. 120 (1973) 1096.
[22] H. Habazaki, P. Skeldon, K. Shimizu, G.E. Thompson, G.C. Wood, J. Phys. D 28 (1995) 2612.
[23] H. Habazaki, M. Uozumi, H. Konno, K. Shimizu, S. Nagata, K. Asami, K. Matsumoto, K. Takayama, Y. Oda, P. Skeldon, G.E. Thompson, Electrochim. Acta 28 (2003) 3257.
[24] G. Amsel, D. Samuel, J. Phys. Chem. Solids 23 (1962) 1707.
[25] N.F. Mott, Philos. Mag. B 55 (1987) 117.
[26] M.-H. Wang, K.R. Hebert, J. Electrochem. Soc. 146 (1999) 3741.
[27] J.A. Davies, B. Domeij, J.P.S. Pringle, S. Brown, J. Electrochem. Soc. 112 (1965) 675.